COVID-19 immunotherapy
A mathematical model

J N Tavares*and Emilie Gomes†
Faculty of Sciences of University of Porto, Portugal
Center of Mathematics of University of Porto
Statistics, Modeling and Computing Applications Office

June 22, 2022

Abstract

The pandemic caused by SARS-CoV-2 is responsible for a terrible health devastation with profoundly harmful consequences for the economic, social and political activities of communities on a global scale. Extraordinary efforts have been made by the world scientific community, who, in solidarity, shared knowledge so that effective vaccines could be produced quickly. However, it is still important to study therapies that can reduce the risk, until group immunity is reached, which, globally, will take a time that is still difficult to predict. On the other hand, the immunity time guaranteed by already approved vaccines is still uncertain. The current study proposes a therapy whose foundation lies in the important role that innate immunity may have, by preventing the disease from progressing to the acute phase that may eventually lead to the patient's death. Our focus is on NK cells and their relevant role.

Natural killer cells (NK) are considered the primary defence lymphocytes against virus-infected cells. They play a critical role in modulating the immune system. Preliminary studies in COVID-19 patients with severe disease, suggest a reduction in the number and function of NK cells, resulting in decreased clearance of infected and activated cells and unchecked elevation of inflammation markers that damage tissue. SARS-CoV-2 infection distorts the immune response towards a highly inflammatory phenotype. Restoring the effector functions of NK cells has the potential to correct the delicate immune balance needed to effectively overcome SARS-CoV-2 infection.

1 Preliminaries. Biological information.

The prevention and control of virus infections involves a complex interplay between diverse cell types of the innate and adaptive immune systems. Natural

*Faculty of Sciences of University of Porto, Portugal, https://sigarra.up.pt/fcup/en/WEB_PAGE.INICIAL. mailto:jntavar@fc.up.pt, Homepage:https://cmup.fc.up.pt/cmup/cv/

†Work supported by GEMAC - https://cmup.fc.up.pt/cmup/gemac/ - Statistics, Modeling and Computing Applications Office. FCUP.

killer cells (NKs) are a type of innate lymphoid cell that play an important role in immune defense against infection in both mice and humans. The contribution of NK cells to cytolytic killing of virus-infected cells is well-established and well-described in immunology textbooks (see [12],[15],[13],[32]).

Likewise, the importance of early and potent production of pro-inflammatory cytokines like interferon gamma (IFN-γ) by NK cells is widely accepted. More recently, there is increasing evidence that NK cells play a key regulatory role in shaping adaptive immune responses to control infection. Nevertheless, NK cells also have been shown to kill both APC (antigen-presenting cells) and virus-specific T-cells, producing anti-inflammatory cytokines, like interleukin-10 (IL-10), suppressing immunity.

Finally, a series of recent intriguing studies have questioned the innate nature of NK cells by advancing the concept of long-lived memory NK cells that can contribute to viral control during latent infections or following re-infection. In fact, NK cells serve to contain virus infections, while the adaptive immune response is generating antigen-specific cytotoxic T-cells (CTLs), and antibodies (Abs) that can clear the infection.

According to Zheng & al. [1], the total number of NK and CD8+T cells (CTL) was decreased markedly in patients with SARS-CoV-2 infection. The function of NK and CTLs was exhausted with the increased expression of NKG2A in COVID-19 patients. NKG2A is a self-inhibitory receptor on NK cells, that suppress their killing activity. On the other hand, patients convalescing after therapy, the number of NK and CD8+T was restored with reduced expression of NKG2A. These results suggest that the functional exhaustion of cytotoxic lymphocytes is associated with SARS-CoV-2 infection. Hence, SARS-CoV-2 infection may break down antiviral immunity at an early stage. We postponed the discussion, and a possible explanation of this phenomenon to section 4.

This means that it is essential that, in the face of a COVID-19 virus attack, the innate immune response must be sufficiently effective, and that, in particular, the number of NK active cells is high up to the point of triggering the elimination of infected cells and also stimulate the action of macrophages and the differentiation of T-cells into CTL cells specific for the virus-associated antigen.

There is, however, another side of the coin. While cytokines and chemokines are important in the immune control of virus infections, their contribution can be harmful as they can potentiate an acute fatal phase of infection called cytokine storm syndrome (CSS) (see [4], [5], [6]), which has been identified as one of the possible causes of death in COVID-19 patients. CSS is a form of systemic inflammatory response syndrome that occurs when large numbers of white blood cells, including B-cells, T-cells, NK's, macrophages, dendritic cells, and monocytes are activated and release inflammatory cytokines, which activate more white blood cells in a positive feedback loop of pathogenic inflammation.

A vast body of evidence provides support to a central role of promotion of massive inflammatory infiltrates with significantly higher levels of cytokines (IFN-γ, TNF-α, IL-1, IL-6, IL-12, IL-18), and chemokines (MIP-2, MIP-1a/b, MCP-1), causing hypercytokinemia [1]. Therefore, particularly early on, potent

[1] potentially fatal immune reaction, consisting of a positive feedback loop between cytokines

inflammatory antiviral activity may be dangerous to the host, rather than protective, due to the deleterious impact on lung pathology.

The aim of this work is essentially to study the role of innate immunity in fighting infection and, in particular, the role of NK cells. In a later study, already underway, we will complement the model considering adaptive immunity in the acute phase of the infection, with the possible appearance of cytokine storm (CSS).

2 Strategies to Enhance NK Cell Function for the Treatment of Infections

Blockade of immune checkpoints. NKG2A blocking.

Among the most promising approaches to immunotherapy is the blockade of immune checkpoints (see [14]). Immune checkpoints refer to inhibitory pathways hardwired into the immune system that are crucial for maintaining self-tolerance and for modulating the duration and amplitude of physiological immune responses in peripheral tissues in order to minimize collateral tissue damage. This has been studied mainly in cancer immunotherapy since it is now clear that tumors choose certain immune-checkpoint pathways as a major mechanism of immune resistance, particularly against T-cells that are specific for tumor antigens [14].

Haanen et al. [3] examine targeting of a novel immune checkpoint, NKG2A, that can be expressed on both NK cells and on CD8+T, as we will see in a moment. NK cells are essential in the early immune response against viral infections, in particular through clearance of virus-infected cells. Let us detail this point.

One key aspect of NK cell function is their ability to kill cells that have down-regulated MHC-I, a process known as missing-self recognition. As NK cells express self-inhibitory receptors that bind to MHC-I molecules, cells with down-regulated MHC-I activate NK cells and become targets of NK cell-mediated cytotoxicity (see Fig. 1).

NK cells defend against viruses or other pathogens, because they are able to distinguish infected cells from uninfected healthy cells ([32], [13],[12]). In fact, NK cells distinguish infected and stressed cells from healthy normal cells, and NK cell function is regulated by a balance between signals that are generated from inhibitory receptors (ex. NKG2A) and activating receptors (ex. NKG2D). These receptors recognize molecules on the surface of other cells and generate inhibitory or activating signals that inhibit or promote NK responses (see Fig. 1). The activating receptors stimulate protein kinases that phosphorylate downstream signaling substrates, while inhibitory receptors stimulate phosphatases that counteract the kinases. In general, the inhibitory receptors recognize ligands on healthy normal cells (Fig. 1(A)), while activating receptors recognize ligands on infected and injured cells (Fig. 1(B)). But, be warned, there is a

and immune cells, with highly elevated levels of various cytokines.

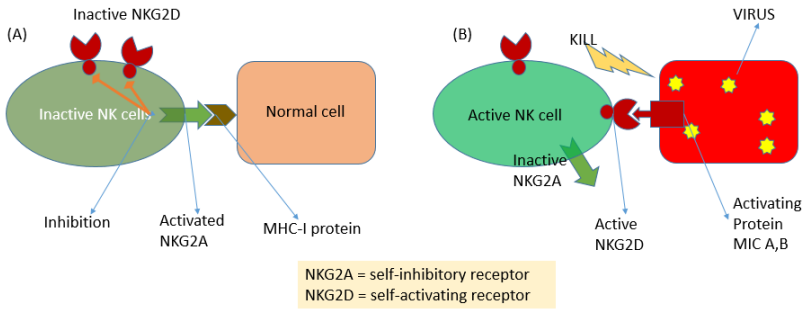

Figure 1: How an *NK* cell recognizes its target. An NK cell preferentially attacks infected host cells because these cells have on their surface both activating proteins (MIC-A,B) and, in some cases, abnormally low levels of MHC-I proteins. (A) - the high levels of MHC-I proteins, found on normal host cells, activate self-inhibitory receptors on the NK cell (ex. NKG2A) that suppress their killing activity. (B): in contrast, the activating proteins on infected cells bind to self-activating receptors on the NK cell (ex. NKG2D) and stimulate their killing activity.

possible violation of this rule. In fact, SARS-CoV-2 can contradict this rule as a self-defense mechanism (see section 4).

As we know, NK cells are able to eliminate virally infected cells in an antigen-independent manner. In fact, NK cells are activated and respond to a variety of different stimuli, including stress-induced proteins, mismatched MHC-I, and missing/down-regulated MHC-I [7]. Viral infections have developed evasion tactics to avoid T-cell recognition. While T-cells and B-cells possess a single antigen receptor that dominates their development and activation, and signals initiated through these antigen receptors are augmented by costimulatory molecules, NK cells, in contrast, do not possess one dominant receptor, but instead rely on a vast combinatorial array of receptors to initiate effector functions.

Cytokine activation of NK-cells

Another important function of NK cells is the production of inflammatory cytokines, such as interferon-gamma (IFN-γ) and tumor necrosis factor alpha (TNF-α). These cytokines recruit T-cells to the site of infection and impact the function and maturation of myeloid cells. The time course of viral infection can be seen in Fig. 2, adapted from [13].

Interferons (IFNs) are a family of cytokines that have been identified through their central role in response to viral infections. In particular, IFN-γ is a cytokine that plays a central role in immune system signaling, modulating innate and adaptive immune responses to viral and bacterial challenges. IFN-γ is secreted predominantly by T-cells and NK cells. IFN-γ signals as an antiparallel homodimer through the high-affinity (IFN-R1) and low-affinity (IFN-R2) receptors. These receptors are present on a very wide range of immune system and other cells, including CD4+ and CD8+ T cells, B-cells, NK cells, dendritic cells (DCs), macrophages, platelets, and others.

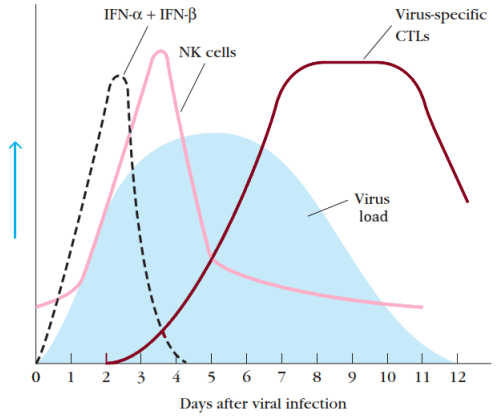

Figure 2: Time course of viral infection. IFN-α, IFN-β, and the cytokines TNF-α and IL-12 are released from virus-infected cells soon after infection (dashed curve). These cytokines stimulate the NK cells, quickly leading to a rise in the NK-cell population (rose curve) from the basal level, which together control virus replication but do not eliminate the virus. NK cells help contain the infection during the period required for generation of CTLs (brown curve). Virus elimination is accomplished when virus-specific CD8+T and neutralizing antibodies are produced. Without NK cells, the levels of some viruses are much higher in the early days of the infection, and the infection can be lethal unless treated vigorously with antiviral compounds. Figure adapted from [13]. The blue shaded region represents Viral load (also known as Viral titer) – a numerical expression of the quantity of virus in a given volume of plasma.

Production and release of IFN-γ by NK cells is typically stimulated by the combination of IL-12 and IL-18. Also in CD8+ T cells and CD4+ T helper cells the combination of IL-12 and IL-18 promotes production and release of IFN-γ (see Fig. 4). It is important to note that neither IL-12 nor IL-18 alone are sufficient to induce elevated production of IFN-γ from NK cells.

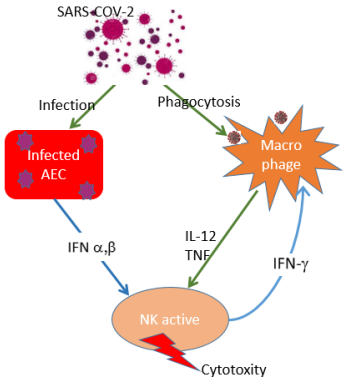

Figure 3: Cytokine activation of NK-cells. Adapted from [32].

The ability of NK cells to kill target cells can be enhanced by interferons or certain cytokines. NK cells capacity of killing infected cells is increased 20– to 100–fold when NK cells are exposed to IFN-α and IFN-β, or to IL-12, a cytokine produced by dendritic cells and macrophages during infection by many types of pathogens. IL-12, acting in synergy with the cytokine IL-18, produced by

activated macrophages, can also stimulate NK cells to secrete large amounts of interferon IFN-γ, and this is crucial in controlling some infections before the IFN-γ produced by activated CTL (CD8+T-cells) becomes available. E. Prompetchara et al. [20], describes a study of 41 hospitalized patients with high-levels of proinflammatory cytokines, including IL-2, IL-7, IL-10, and TNF-α observed in the COVID-19 severe cases. These findings are in line with SARS in that the presence of lymphopenia (abnormally low level of lymphocytes in the blood) and cytokine storm syndrome (CSS) may have a major role in the pathogenesis of COVID-19. This CSS can initiate viral sepsis and inflammatory-induced lung injury which lead to other complications including pneumonitis, acute respiratory distress syndrome (ARDS), respiratory failure, shock, organ failure and potentially death.

Several unrelated viruses, including influenza virus, respiratory syncytial virus, and human immunodeficiency virus, can directly interfere with NK cell functionality, through infection of these cells. Viral infection can lead to immune suppression, either by downregulation of the cytotoxic function or by triggering apoptosis, leading to depletion of NK cells.

On the other hand, a vast body of evidence provides support to a central role of exaggerated production of IFN-γ in causing hypercytokinemia and signs and symptoms of HLH[2].

3 Mathematical Modeling

Our model will focus in the role of innate immunity (cells and cytokines included), in fighting infection and, in particular, the role of NK cells. Figure 4 shows a schematic diagram of the proposed model dynamics and the associated equations are given in the text. The ODE's modeling methodology owes much to previous work by Avner Friedman [34], Ruby Kim [45], Ami Radunskaya [67], Denise Kirschner [47], among others. Specifically, we use (i). the distinction between internal virus load V_{int}, within infected cells, and external or free virus load V_{free}, (ii). Hill's kinetic laws to model activation/inhibition factors, (iii). parameter values due to the lack of experimental data. The significance, units and simulation values of the parameters used in the equations below, can all be seen in section 8.

Previous studies have shown that SARS-CoV-2 predominantly infects airway and alveolar epithelial cells (AECs) and macrophages. SARS-CoV-2 uses the same entry receptor, angiotensin-converting enzyme (ACE2), as SARS-CoV, for infection, suggesting the likelihood of the same set of cells being targeted and infected. We start with a classic viral dynamic model, with eclipse phase [19], [36], where: (i). Target Cells (AECs) that are susceptible to infection, A_0, become infected, (A_I), upon interaction with infectious free viral particles, V_{free}, at rate $\beta_1 V_{\mathsf{free}}$, according to mass–action law, where β_1 is the infection rate constant; (ii). Target cells, A_0, have a constant supply rate, s, and natural

[2]Hemophagocytic lymphohistiocytosis (HLH), is a life-threatening disease of severe hyperinflammation characterized by proliferation of morphologically benign lymphocytes and macrophages that secrete high amounts of inflammatory cytokines. It is classified as one of the cytokine storm syndromes

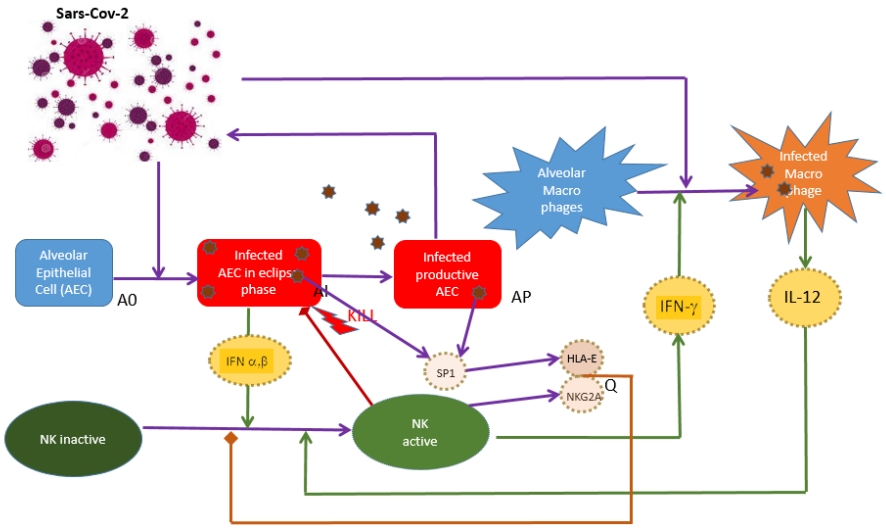

Figure 4: Schematic diagram of viral dynamics and innate response.

death rate, μ; (iii). An eclipse phase, in which A_I cells remain infected, the virus is replicated in the usual way, but not yet released into the plasma. These infected cells evolve into a productive state, A_P, in which they explode, releasing virions at the rate p virions/cell. (iv). Virus is cleared at rate c per virion, which corresponds to a half-life $t_{1/2} = \ln(2)/c$, and (v). An infected cell has an average lifespan of $1/\delta$, where δ is its death rate, and thus produces an average of $p_m = p/\delta$ virions during its lifetime. Infected cells (A_I) can be killed by interaction with active Natural Killers (N_{at}) (see [5], [6]), and so we have the following first three equations (See Fig. 4):

$$\frac{dA_0}{dt} = s - \beta_1 A_0 \cdot V_{\mathsf{free}} - \mu A_0 \tag{1}$$

$$\frac{dA_I}{dt} = \underbrace{\beta_1 A_0 \cdot V_{\mathsf{free}}}_{\text{Infection}} - \underbrace{\beta_2 N_{\mathsf{at}} \cdot A_I}_{\text{Killing}} - \delta A_I \tag{2}$$

$$\frac{dA_P}{dt} = \delta A_I - \underbrace{\beta_2 N_{\mathsf{at}} \cdot A_P}_{\text{Killing}} - \eta A_P \tag{3}$$

We have assumed a constant supply of A_0-cells, like in [47]. We distinguish between two populations of virus: free virus, V_{free}, in plasma, and internal virus, V_{int}, in alveolar and macrophages infected cells. We neglect the internal virions in infected macrophages that are killed by phagocytosis. The equation for the free virus, has a term coming from the bursting of A_P-cells, with burst number p virions/A_P. V_{int} have terms corresponding to virus proliferation in A_I and A_P cells, and subtracting terms corresponding to killing of A_I and A_P cells by activated NK–cells, N_{at}.

$$\frac{dV_{\mathsf{free}}}{dt} = \underbrace{\eta \cdot p \cdot A_P \cdot \vartheta^m_{\mathsf{int}}}_{\text{Bursting}} - \beta_1\, A_0 \cdot V_{\mathsf{free}} - \beta_4\, M_0 \cdot V_{\mathsf{free}} - c\, V_{\mathsf{free}} \tag{4}$$

$$\frac{dV_{\mathsf{int}}}{dt} = \underbrace{r\, V_{\mathsf{int}}(1-\vartheta^m_{\mathsf{int}})}_{\substack{\text{Virus proliferation}\\ \text{in } A_P \text{ and } A_I\text{-cells}}} + \underbrace{\beta_1\, A_0 \cdot V_{\mathsf{free}}}_{V_{\mathsf{free}} \to V_{\mathsf{int}}} + \underbrace{\beta_4\, M_0 \cdot V_{\mathsf{free}}}_{V_{\mathsf{free}} \to V_{\mathsf{int}}}$$
$$-\eta \cdot p \cdot A_P \cdot \vartheta^m_{\mathsf{int}} - \underbrace{p_1\, \beta_2\, N_{\mathsf{at}} \cdot (A_I + A_P) \cdot \vartheta^m_{\mathsf{int}}}_{\substack{\text{Killing of } V_{\mathsf{int}} \in A_I \cup A_P\\ \text{before bursting}}} \tag{5}$$

where we have defined $\vartheta^m_{\mathsf{int}}$ by

$$\vartheta^m_{\mathsf{int}} = \left(\frac{V^m_{\mathsf{int}}}{V^m_{\mathsf{int}} + (p\, A_P)^m}\right)$$

Here $p_1 < p$, and we assume that, in the average, $p_1 = (p/2)$ $\mathsf{virions}/A_I, A_P$.

Inactive NKs (Natural Killer cells), N_{in}, are activated through the positive mediation of Interferons IFN-$\boldsymbol{\alpha}$ and IFN-$\boldsymbol{\beta}$, $I_{\alpha,\beta}$, which, in turn, are segregated by infected AECs, A_I and A_P. Moreover the activation of NKs is also stimulated be cytokine IL-12, I_{12}, which, in turn, are segregated by infected alveolar macrophages, M_I (see Fig. 4). On the other side, as we have said before, SARS-CoV-2 defends itself, inactivating active NK cells, presumably, increasing the cytoxity self-inhibitor NKG2A, as we will see soon. Therefore, we obtain four more equations:

$$\frac{dN_{\mathsf{at}}}{dt} = \underbrace{k_1\, N_{\mathsf{in}} \cdot \left(\frac{I_{\alpha\beta}}{K_{\alpha\beta} + I_{\alpha\beta}}\right)}_{\substack{I_{\alpha\beta}\text{-activated}\\ \text{production of } N_{\mathsf{at}}\text{-cells}}} + \underbrace{k_2\, N_{\mathsf{in}} \cdot \left(\frac{I_{12}}{K_{12} + I_{12}}\right)}_{\substack{I_{12}\text{-activated}\\ \text{production of } N_{\mathsf{at}}\text{-cells}}} +$$
$$-\beta_2\, N_{\mathsf{at}} \cdot (A_I + A_P) - \mu_1\, N_{\mathsf{at}} \tag{6}$$

$$\frac{dN_{\mathsf{in}}}{dt} = k_3 - k_1\, N_{\mathsf{in}} \cdot \left(\frac{I_{\alpha\beta}}{K_{\alpha\beta} + I_{\alpha,\beta}}\right) +$$
$$-k_2\, N_{\mathsf{in}} \cdot \left(\frac{I_{12}}{K_{12} + I_{12}}\right) - \mu_2\, N_{\mathsf{in}} \tag{7}$$

$$\frac{dM_I}{dt} = \underbrace{k_4\, M_0 \cdot \left(\frac{I_\gamma}{K_\gamma + I_\gamma}\right)}_{\substack{I_\gamma\text{-activated}\\ \text{production of } M_I\text{-cells}}} + \underbrace{\beta_4\, M_0 \cdot V_{\mathsf{free}}}_{\text{Infection}} - \mu_3\, M_I \tag{8}$$

$$\frac{dM_0}{dt} = k_0 - k_4\, M_0 \cdot \left(\frac{I_\gamma}{K_\gamma + I_\gamma}\right) - \beta_4\, M_0 \cdot V_{\mathsf{free}} - \mu_4\, M_0 \tag{9}$$

The equation for IL-12 is

$$\frac{dI_{12}}{dt} = k_{12}\, M_I - \mu_{12}\, I_{12} \tag{10}$$

IFN-$\boldsymbol{\gamma}$, I_γ, is produced by active NK cells, N_{at}:

$$\frac{dI_\gamma}{dt} = k_\gamma\, N_{\mathsf{at}} - \mu_\gamma\, I_\gamma \tag{11}$$

Similarly, IFN-$\boldsymbol{\alpha}$ and IFN-$\boldsymbol{\beta}$, $I_{\alpha\beta}$, are produced by A_I and A_P, and this production is activated by V_{int}:

$$\frac{dI_{\alpha\beta}}{dt} = k_{\alpha\beta}\,(A_I + A_P)\cdot \vartheta^m_{\mathsf{int}} - \mu_{\alpha\beta}\, I_{\alpha,\beta} \tag{12}$$

4 Inhibition of NK cytoxity by the complex NKG2A/HLA-E

As a self–inhibitory receptor, NKG2A has been demonstrated to induce NK cell exhaustion in chronic viral infections. Notably, NKG2A expression, on NK and CD8+T-cells, results in functional exhaustion of NK and CD8+T-cells. In patients infected with SARS-CoV-2, NKG2A expression was increased significantly on NK and CD8+T cells compared with that in HCs (healthy controls). Thus, blocking NKG2A, releases both T-cell and NK cell effector functions. In fact, André et al. [2] shows that blocking the inhibitory NKG2A receptor enhances both natural killer (NK) and CTL (CD8+T) effector functions in mice and humans.

In an interesting study, Daria Bortolotti and collaborators [55] evaluated the possible role of SARS-CoV-2 spike proteins in modifying NK cell functions. Their conclusion is that SARS-CoV-2 Spike 1 Protein (SP1), when presented by infected lung epithelial cells, A_I and A_P, via HLA-E molecules, modifies NK Cell cytotoxicity. They successfully test the hypothesis that the resulting inactivity of NK cells to kill A_I and A_P cells, expressing SP1, was determined by HLA-E/NKG2A binding. They evaluated the effect of SARS-CoV-2 spike proteins in the control of NK cell activation, considering SP1, which is involved in the attachment of the virion to the cell membrane by interacting with ACE2 receptor, and SP2 that mediates the fusion of the virion.

As Bortolotti [55] shows, since the presence of intracellular SP1 protein in lung epithelial cells induced a decrease in the cytotoxic activity of NK cells, we analyzed the possible factors involved in the modification of NK cell status. Since viral proteins are commonly recognized and degraded by the proteasome inside the infected cells, we hypothesized that SP1 peptides might be presented to NK cells. Intracellular peptide presentation is performed by human leukocyte antigen (HLA) class I molecules, which are expressed by all nucleated cells. Epithelial lung cells can express also non-classical HLA-E molecule. HLA-E binds peptides primarily derived from specific signal sequences and interacts with NKG2A/CD94 NK cell inhibitory receptors. There was a significant increase in HLA-E protein and mRNA expression in the presence of SP1 protein.

Denote by N the concentration of NKG2A protein, in N_{at}-cells, H the concentration of $H = \mathsf{HLA\text{-}E}$ protein, in $A_I \cup A_P$-cells, and finally Q (the concentration of) the complex

$$Q = \mathsf{NKG2A/HLA\text{-}E}$$

More concretely HLA-E is induced by SP1 protein of internal virions on infected alveolar cells A_I and A_P (see below). $N = \mathsf{NKG2A}$ is expressed on the surface of activated NK cells, N_{at}-cells. Hence, N is given by

$$N = \rho_N \, N_{\mathsf{at}} \tag{13}$$

where ρ_N is the ratio between the mass of one N–protein to the mass of one N_{at} cell. Now, $H = \mathsf{HLA\text{-}E}$ is expressed on the surface of infected A_I and A_P cells. Following the conclusion of [55], SARS-CoV-2 Spike 1 Protein (SP1), when presented by infected lung epithelial cells, A_I and A_P, via HLA-E molecules, modifies NK Cell cytotoxicity. Hence, the concentration H of HLA-E is up-regulated by V_{int}. We assume that its dynamics follows the ODE:

$$\frac{dH}{dt} = \rho_H \, r \, V_{\mathsf{int}} \cdot (1 - \vartheta_{\mathsf{int}}^m) - \mu_H \, H - k_Q \, \rho_N N_{\mathsf{at}} \cdot H - k_Q \, \rho_N \, (N_{\mathsf{at}} \cdot H) \cdot \mathsf{Inhib}_Q \tag{14}$$

The complex Q results from the reaction $N + H \xrightarrow{k_Q} Q$, which leads to mass–action equation:

$$\frac{dQ}{dt} = k_Q \, \rho_N \, N_{\mathsf{at}} \cdot H \tag{15}$$

This $Q = \mathsf{NKG2A/HLA\text{-}E}$ complex inhibits the activation $N_{\mathsf{in}} \longrightarrow N_{\mathsf{at}}$, by a **Hill factor** Inhib_Q, defined by:

$$\mathsf{Inhib}_Q = \frac{K_Q^m}{K_Q^m + Q^m} \tag{16}$$

since NKG2A is a self-inhibitor of of NK cytoxity. We model the inhibition effect of Inhib_Q, by Hill's law, as usual (see [34], [47]). As $\mathsf{Inhib}_Q = \dfrac{1}{1 + (Q/K_Q)^m}$, the constant K_Q is the half-saturating, in the sense that when $Q \to K_Q$, $\mathsf{Inhib}_Q \to 1/2$. When $Q \to \infty$, $\mathsf{Inhib}_Q \to 0$ (max inhibition) and when $Q \to 0$, $\mathsf{Inhib}_Q \to 1$ (no inhibition). Hence equation (6) for dN_{at}/dt, must be modified by:

$$\begin{aligned} \frac{dN_{\mathsf{at}}}{dt} \quad = \quad & k_1 \, N_{\mathsf{in}} \cdot \left(\frac{I_{\alpha\beta}}{K_{\alpha\beta} + I_{\alpha\beta}} \right) \cdot \mathsf{Inhib}_Q + \\ & + k_2 \, N_{\mathsf{in}} \cdot \left(\frac{I_{12}}{K_{12} + I_{12}} \right) \cdot \mathsf{Inhib}_Q + \\ & - \beta_2 \, N_{\mathsf{at}} \cdot (A_I + A_P) - \mu_1 \, N_{\mathsf{at}} \end{aligned} \tag{17}$$

5 Treatment with NKG2A–blocker

The new aspects of interaction between SARS-CoV-2 SP1 protein and the host cells, described in the previous section, might have important implications in the

pathogenesis of COVID-19, providing opportunities for developing new therapies against SARS-CoV-2. In particular, counteracting the cellular stress, targeting the SP1 protein or using NKG2A–blockers, might represent new strategies to enhance the innate immune response at the early stage of the disease, inducing mucosal immunity that might lead to a long-term protection against infection.

Monalizumab is a monoclonal antibody developed to bind to NKG2A receptors expressed on T and NK cells, which could reestablish a broad anti-viral response. It is a checkpoint inhibitor. The natural ligand of NKG2A is HLA-E (HLA class I histocompatibility antigen, alpha chain E), which is frequently over-expressed in tumor diseases, transplants and virus-infected. Binding of HLA-E to NKG2A leads to the inhibition of activation and cytotoxic activity of T and NK cells.

The antibody drug Monalizumab is aimed at blocking the binding of NKG2A to HLA-E, and thus activate T and NK cells and their cytotoxic cell responses, enhancing the immune function of the body and re-establishing their immune response. In fact, blocking the binding of NKG2A to HLA-E, inhibits the Q-inhibitor of activation $N_{\mathsf{in}} \longrightarrow N_{\mathsf{at}}$, and so enhances NK cytoxity.

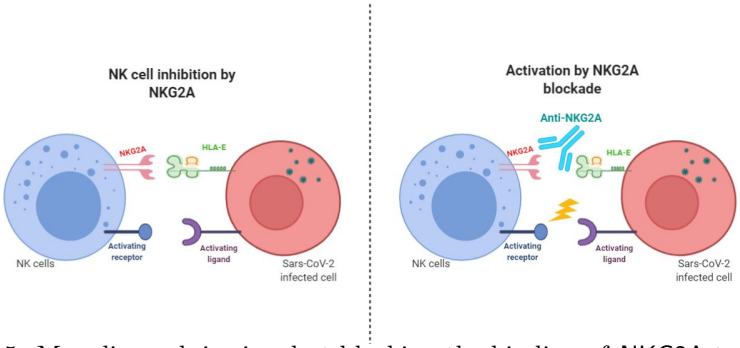

Figure 5: Monalizumab is aimed at blocking the binding of NKG2A to HLA-E.

Equation for NKG2A–blocker Monalizumab

We assume that Monalizumab is injected intradermally in three doses, in days 2, 16 and 30, by an amount of $\theta\,\mathsf{pg/mL}$ (the effective dose level of the drug), providing a source I_θ:

$$I_\theta(t) = \begin{cases} \theta & \text{if} \quad 2 \le t \le 3 \\ \theta & \text{if} \quad 16 \le t \le 17 \\ \theta & \text{if} \quad 30 \le t \le 31 \\ 0 & \quad \text{otherwise} \end{cases} \tag{18}$$

and a corresponding concentration M_θ, given by:

$$\frac{dM_\theta}{dt} = I_\theta(t) - \delta_M\, M_\theta - k_B\, \rho\, (N_{\mathsf{at}} \cdot M_\theta) \tag{19}$$

Let B_θ be the complex $B_\theta = M_\theta/\mathsf{NKG2A}$, that results from the process of NKG2A-blocking:

$$N + M_\theta \xrightarrow{k_B} B_\theta$$

which leads to mass–action equation:

$$\frac{dB_\theta}{dt} = k_B\, N \cdot M_\theta = k_B\, \rho_N\, (N_{\mathsf{at}} \cdot M_\theta) \tag{20}$$

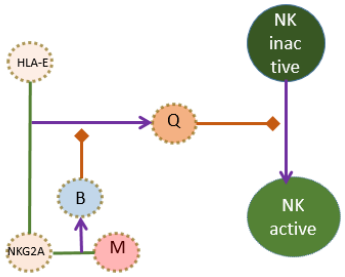

Figure 6: Treatment with NKG2A–blocker B.

As we said before, Monalizumab, or any other NKG2A-blocker, is aimed at blocking the binding of NKG2A to HLA-E, and this is achieved by blocking NKG2A. We model this effect by a **Hill factor** Inhib_B, defined by:

$$\mathsf{Inhib}_B = \frac{K_B^m}{K_B^m + B^m} \tag{21}$$

which inhibits Q, and thus activate NK cells and their cytotoxic response. Under treatment the equation (15) for Q, must be modified by the following one:

$$\frac{dQ}{dt} = k_Q\, \rho_N\, (N_{\mathsf{at}} \cdot H) \cdot \mathsf{Inhib}_B \tag{22}$$

Conclusion: Under treatment we have a new system of differential equations, formally equal to the "control" system (without treatment), but with new variables, $A_0(\theta), A_I(\theta), A_P(\theta), N_{\mathsf{at}}(\theta)$, and so one. The equations are

- Final equations without treatment: Equations (1) to (12), with (6) substituted by (17), tacking account of the inhibition, by SARS-CoV-2 virus, of NK-activation.
- Final equations with M-treatment: formally, the same as before, with new variables as we have said above, where, for simplicity we omit the θ-dependence, with (15), for Q, substituted by (22), tacking account of the inhibition, by the blocker B, of Q-activation, together with equations (19) for M, and (20) for B. We must subtract the terms $k_B\,(\rho N_{\mathsf{at}} \cdot M_\theta)$ and $k_Q\,(\rho_N N_{\mathsf{at}} \cdot H) \cdot \mathsf{Inhib}_B$, in the N_{at}-ODE (17), to guarantee mass conservation. Therefore, the final equation for N_{at}, under treatment, must be:

$$\begin{aligned}\frac{dN_{\mathsf{at}}}{dt} \;=\; & k_1\, N_{\mathsf{in}} \cdot \left(\frac{I_{\alpha\beta}}{K_{\alpha\beta} + I_{\alpha\beta}}\right) \cdot \mathsf{Inhib}_Q + k_2\, N_{\mathsf{in}} \cdot \left(\frac{I_{12}}{K_{12} + I_{12}}\right) \cdot \mathsf{Inhib}_Q + \\ & -\beta_2\, N_{\mathsf{at}} \cdot (A_I + A_P) - \mu_1\, N_{\mathsf{at}} - k_B\,(\rho_N N_{\mathsf{at}} \cdot M_\theta) + \\ & -k_Q\,(\rho_N N_{\mathsf{at}} \cdot H) \cdot \mathsf{Inhib}_B \end{aligned} \tag{23}$$

6 Simulations and Results

We have used the software COPASI `http://copasi.org/`, for numerical integration of our equations. The parameters were found through a detailed revision of the bibliography. Some of them were adjusted to reproduce more faithful the already known dynamics of SARS-CoV-2 virus load (VL, without treatment with NKG2A-blockers, as far as we know).

This type of modeling, by ignoring the spatial component, as well as factors intrinsically stochastic to the molecular regimens, implies a very drastic simplification of the complexity of biological phenomena at the cellular and molecular scale. However, they can be useful as first approximations and, in any case, they provide an alternative in silico simulation process, with the advantage of being able to lead to simulations of quantifiable observable dynamics, as well as possible control through appropriate therapies.

The paradigm of immunotherapy treatment, in this case of the NKG2A/HLA-E checkpoint blocking, seems very promising for effective therapies for SARS-CoV-2, preventing the disease from evolving to severe acute states. As we have already said, this work must be deepened, taking into account the decisive role of the adaptive immune system and consideration of the serious risk factor - the cytokine storm.

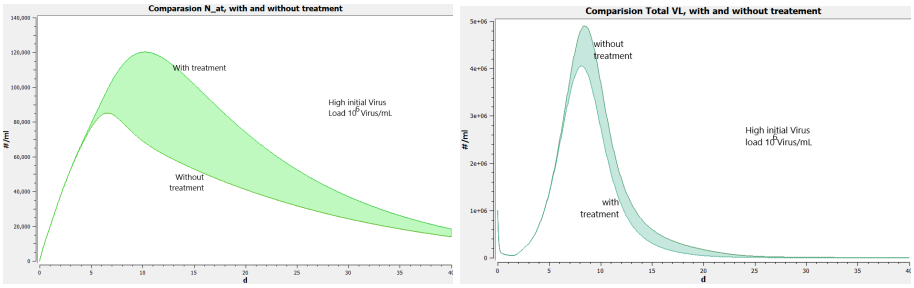

Figure 7: N_{at} **and total Viral load evolution, for high initial V** $\approx 10^6$ **virions/mL.** Note that the peak of N_{at} population, with blocking treatment, is much higher than the peak of the N_{at} population, without treatment, in the situation of high viral load ($\approx 10^6$ virions/mL. The peak of N_{at}, with treatment is reached for 120.000virions/mL against about 80.000 without treatment. An increase of about 50%. The delay is about 4 days. This increase in N_{at} corresponds to a decrease in the total viral load with treatment, which may have an impact on the progression of the disease to more acute states, namely the uncontrolled production of cytokines eventually leading to CSS.

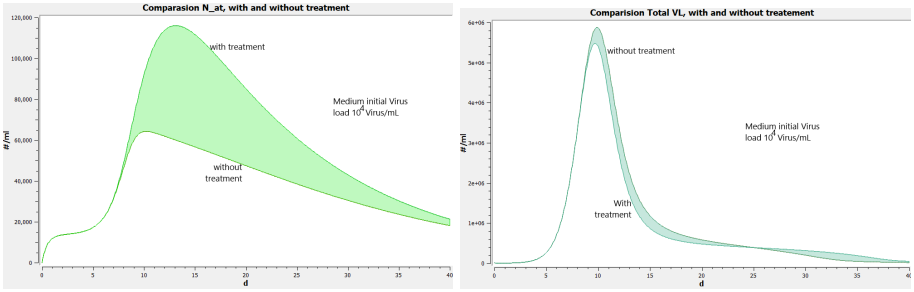

Figure 8: N_{at} **and total Viral load evolution, for medium initial V** $\approx 10^4$ **virions/mL**. Note that the peak of N_{at} population, with blocking treatment, is much higher than the peak of the N_{at} population, without treatment, in the situation of medium viral load ($\approx 10^4$ virions/mL. The peak of N_{at}, with treatment is reached for 120.000virions/mL against about 60.000 without treatment. An increase of about 100%. The delay is about 4 days. This increase in N_{at} corresponds to a decrease in the total viral load with treatment, which may have an impact on avoiding CSS development.

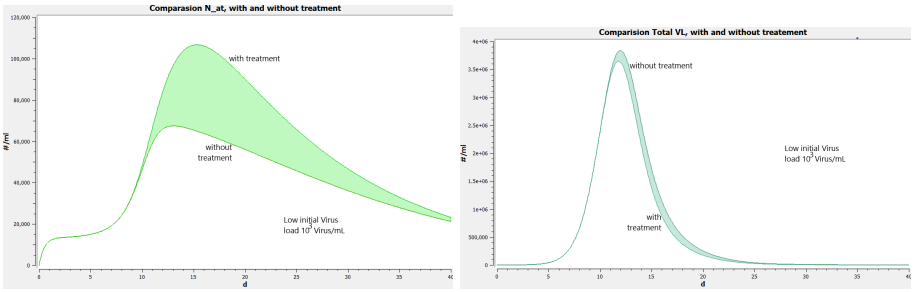

Figure 9: N_{at} **and total Viral load evolution, for low initial V** $\approx 10^3$ **virions/mL.** Similar observations to the two previous figures.

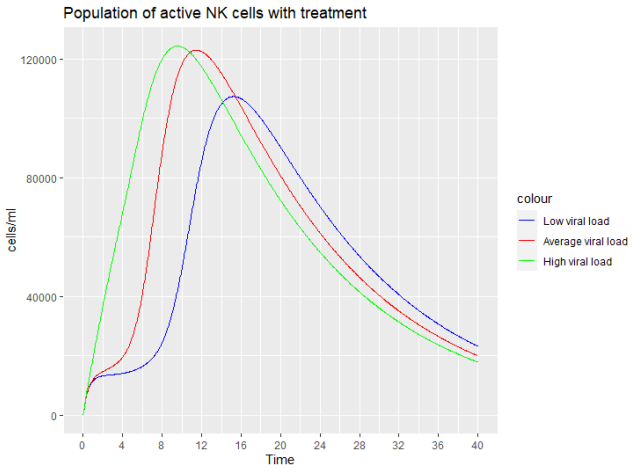

Figure 10: **Comparison of N_{at} cell concentration, with different initial viral loads and treatment. Initial high, medium and low viral loads are 10^6, 10^4 and 1000 virions/mL, respectively.** Regarding the population of N_{at} cells, one of the observations resulting from our simulations, was that, with a high initial viral load, the initial growth of N_{at} was very fast, with a higher peak, than with other viral loads. See text.

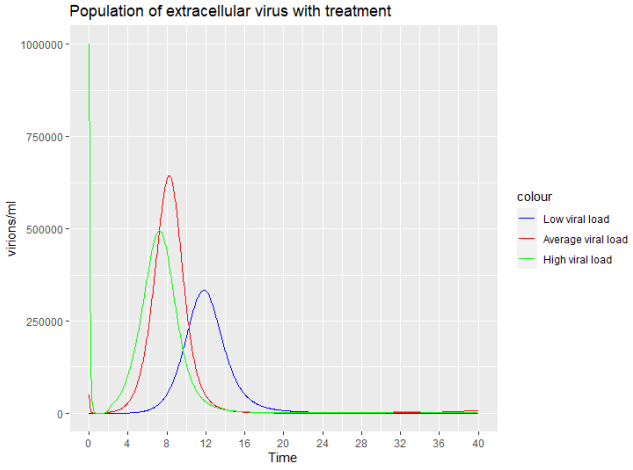

Figure 11: **Comparison of the extracellular virus concentration, V_{free}, with different initial viral loads and treatment. Initial high, medium and low viral loads are 10^6, 10^4 and 1000 virions/mL, respectively.** As for the intra (or extracellular virus in the next figure), it was observed that initially the free virus with high viral load decreases. This may be due to the fact that the virus begins to infect healthy cells and there is a decrease in the extracellular virus and an increase in the intracellular virus. See text.

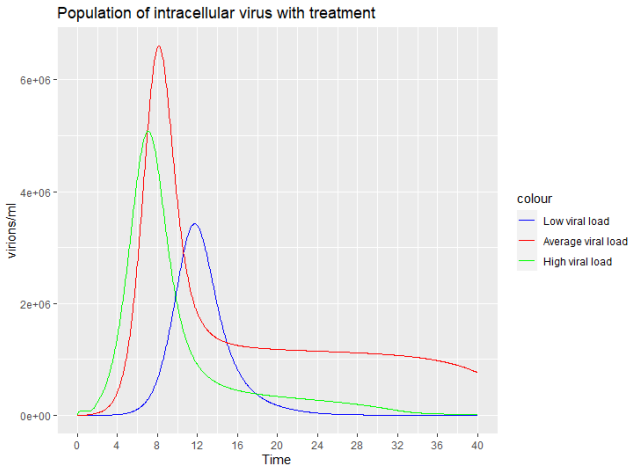

Figure 12: **Comparison of the intracellular virus concentration, V_{int}, with different initial viral loads and treatment**. Initial high, medium and low viral loads are 10^6, 10^4 and 1000virion/mL, respectively.

7 Discussion and conclusions

Regarding the population of active NK cells, one of the observations resulting from our simulations, was that, with a high initial viral load, the initial growth of active NKs was very fast, with a higher peak, than with other viral loads. This is reasonable, since if initially the concentration of virions is very high, they infect healthy cells more quickly, so there are more infected cells and, consequently, the larger the population of active NK cells will be. Another observation was about slowing growth when the viral load was low. This may be due to the fact that the load is very low and the time of infection by the virus is shorter in this case than with higher viral loads.

As for the intra or extracellular virus, it was observed that initially the free virus with high viral load decreases. This may be due to the fact that the virus begins to infect healthy cells and there is a decrease in the extracellular virus and an increase in the intracellular virus.

Note that it was also observed that the virus peak (both extracellular and intracellular) with intermediate initial load exceeds the virus peak when the initial load is high. Although there is no scientific explanation, there is a study that shows that low viral loads cause higher peaks than high viral loads [68]!, which goes according to the results obtained in the simulations of Fig. 6 and Fig. 6.

The model we present in this article is, as far as we know, an unprecedented model regarding the role that innate immunity may play in the early control of the disease, preventing it from reaching more serious states. When considering the two populations of internal viruses, in the infected cells, and the lifespan of these cells until their burst, releasing viruses to the free virus population, V_{free}, the model is more realistic.

In this article, the methodology of blocking receptors to the adhesion of the virus to alveolar cells is developed. A technique similar to the one being developed in the context of cancer treatment by immunotherapy.

In Fadai NT et al. ([69]), a mechanistic ODE model is developed, of hyperinflammation, leading to the so-called cytokine storm (CSS), which many believe is responsible for the most serious stages of the disease.

There are common points to our work. Both treat the earlier stage of the infection. Fadai et al. emphasis is placed on preventing hyper-inflammatory states that lead to cytokines storm (CSS), proposing a preventive treatment that accelerates the clearance of pro-inflammatory cytokines by anti-inflammatories. Specifically, they suggest that "*early intervention with a locally acting anti-inflammatory agent (such as inhaled corticosteroids) may effectively blockade the pathological hyper inflammatory reaction as it emerges*". They also look at other intervention strategies that reduce viral infection of susceptible cells.

Our model is also mechanistic (ODE) but considers more species in population dynamics. In particular, it seems relevant to consider two viral species, V_{int} and V_{free}, and the consideration of latency periods and subsequent burst of infected cells. Our treatment strategy is also completely different from the one proposed in Fadai et al. The strategy we propose is typical of im-

munotherapy, inspired by analogue models in cancer treatment, in this case of the NKG2A/HLA-E checkpoint blocking, which seems very promising for effective therapies for SARS-CoV-2, preventing the disease from evolving to severe acute states. The proposed treatment, through the antibody drug Monalizumab, is aimed at blocking the binding of NKG2A to HLA-E, and thus activate T and NK cells and their cytotoxic cell responses.

Acknowledgments

The first author thanks all the affection, love, support and peace, of his entire family, including cats and dogs. In particular, he would like to thank Dr. José Manuel Poças, from Setúbal Hospital, for his encouragement and helpful advice. The second author thanks all the support, motivation and, above all, patience to all his family.

The authors would like to thank the referees for their valuable suggestions, which greatly valued this work. We are grateful for the reference to the interesting work by Fadai et al. which has common points with our work although, in addition to differences in the species considered in the population dynamics, the treatment methodology is substantially different, as described in the final part of the previous section.

8 Supplementary material

This model was deposited in BioModels ([70]), `https://www.ebi.ac.uk/biomodels`, and assigned the identifier MODEL2109130003.

If you have any access difficulties, please send me an email jntavar@fc.up.pt, so I can return the complete Copasi simulation model.

Given the impossibility of accessing serological data, it makes some sense to follow the main parameters used in previous studies on SARS viruses. However, SARS-CoV-2 has different characteristics that lead to different temporal dynamics and degrees of severity than those mentioned. On the other hand, it is too early to have reliable serological data on SARS-CoV-2. In this context, the parameters were assumed within a logic of plausibility maintaining the parameters of previous studies, namely production and decay rates $\beta_i, \mu_i, etc.$, and some were adjusted to the infection onset and to the most readily accessible observables, namely VL peak, eclipse time, infection time, etc.

We postpone to a future work the simulation with combined treatment with anti-virals like, for example, Remdisivir.

Dynamic variables	Name	Units
A_0	Susceptible epithelial cell	A_0/mL
A_I	Infected epithelial cells	
	in elipse (non-productive) phase	A_I/mL
A_P	Infected epithelial cells	
	in productive phase	A_P/mL
V_{free}	Free virus particles in plasma	$V_{\mathsf{free}}/\mathsf{mL}$
V_{int}	Internal virus particles in $A_I \cup A_P$ cells	$V_{\mathsf{int}}/\mathsf{mL}$
N_{in}	Inactive NK cells	$N_{\mathsf{in}}/\mathsf{mL}$
N_{at}	Active NK cells	$N_{\mathsf{at}}/\mathsf{mL}$
M_0	Macrophages	M_0/mL
M_I	Infected Macrophages	M_I/mL
I_{12}	IL-12	pg/mL
I_γ	IFN-$\boldsymbol{\gamma}$	pg/mL
$I_{\alpha\beta}$	IFN-$\boldsymbol{\alpha}$ $\cup$ IFN-$\boldsymbol{\beta}$	pg/mL
N	NKG2A protein	pg/mL
H	HLA-E protein	pg/mL
Q	Complex NKG2A/HLA-E	pg/mL
M_θ	anti-NKG2A with dose θ	pg/mL
B_θ	Blocking Complex NKG2A/M_θ	pg/mL

Parameters	Description	Units
s	Production rate of susceptible A_0-cells	$(A_0/\mathsf{mL})/\mathsf{day}$
β_1	Virus infection rate of A_0-cells	$(V_{\mathsf{free}}/\mathsf{mL})^{-1}/\mathsf{day}$
μ	Natural death rate of susceptible A_0-cells	day^{-1}
β_2	Killing rate of infected A_I-cells by active NK cells	$(N_{\mathsf{at}}/\mathsf{mL})^{-1}/\mathsf{day}$
δ	Death rate of infected A_I-cells	day^{-1}
η	Death rate of A_P-cells	day^{-1}
p	burst number	$\mathsf{virions}/A_P$
β_4	Virus infection rate of M_0-cells	$(V_{\mathsf{free}}/\mathsf{mL})^{-1}/\mathsf{day}$
c	Virus death rate	day^{-1}
r	Growth rate of internal virus	day^{-1}
k_1	Activation rate of NK cells from N_{in}-cells up-regulated by IFN-$\boldsymbol{\alpha}$ and IFN-$\boldsymbol{\beta}$	day^{-1}
k_2	Activation rate of NK cells from N_{in}-cells up-regulated by IL-12	day^{-1}
k_3	Production rate of N_{in}-cells	$(N_{\mathsf{in}}/\mathsf{mL})/\mathsf{day}$
μ_1	Death rate of N_{at}-cells	day^{-1}
μ_2	Death rate of N_{in}-cells	day^{-1}
$K_{\alpha\beta}$	$I_{\alpha,\beta}$ half-saturation in the positive up-regulation of NK-cell activation	$I_{\alpha,\beta}/\mathsf{mL}$
K_{12}	IL-12 half-saturation in the positive up-regulation of NK-cell activation	I_{12}/mL
K_γ	IFN-$\boldsymbol{\gamma}$ half-saturation in the positive up-regulation of M_0-activation	I_γ/mL
k_4	Activation rate of M_I-cells, from inactive M_0-cells, modified by IFN-$\boldsymbol{\gamma}$	day^{-1}
μ_3	Death rate of M_I-cells	day^{-1}
k_0	Production rate of M_0-cells	(M_0/mL) /day
μ_4	Death rate of M_0-cells	day^{-1}
k_{12}	Production rate of IL-12 by M_I-cells	$(\mathsf{pg}/M_I)/\mathsf{day}$
μ_{12}	Decay rate of IL-12	day^{-1}
k_γ	Production rate of IFN-$\boldsymbol{\gamma}$ by active NK-cells	$(\mathsf{pg}/N_{\mathsf{at}})/\mathsf{day}$
μ_γ	Decay rate of IFN-$\boldsymbol{\gamma}$	day^{-1}
$k_{\alpha\beta}$	Production rate of of IFN-$\boldsymbol{\alpha}$ and IFN-$\boldsymbol{\beta}$ by A_I and A_P-cells	$(\mathsf{pg}/A_{I,P})/\mathsf{day}$
$\mu_{\alpha\beta}$	Decay rate of of IFN-$\boldsymbol{\alpha}$ and IFN-$\boldsymbol{\beta}$	day^{-1}

Table 1: Table with the description of the parameters used in the model of differential equations.

Parameters	Value	Units	References
s	4×10^3	$(A_0/\mathsf{mL})/\mathsf{day}$	[47]
β_1	1.17228×10^{-6}	$(V_{\mathsf{free}}/\mathsf{mL})^{-1}/\mathsf{day}$	[8]
β_2	3.72316×10^{-6}	$(N_{\mathsf{at}}/\mathsf{mL})^{-1}/\mathsf{day}$	adjusted
β_4	2.77351×10^{-7}	$(V_{\mathsf{free}}/\mathsf{mL})^{-1}/\mathsf{day}$	[47]
μ	0.14	day^{-1}	[8]
c	10	day^{-1}	[61]
p	400	$\mathsf{virions}/A_P$	[65]
r	2.5	day^{-1}	[47]
δ	4	day^{-1}	[61]
η	2	day^{-1}	[61]
k_1, k_2	0.52	day^{-1}	[66]
k_0	0	day^{-1}	assumed
k_3	0	$(N_{\mathsf{in}}/\mathsf{mL})^{-1}/\mathsf{day}$	assumed
k_4	0.4	day^{-1}	[47]
μ_1	0.07	day^{-1}	[66]
μ_2	0.0412	day^{-1}	[67]
μ_3	0.05	day^{-1}	[34]
μ_4	0.008	day^{-1}	[34]
k_3	0	day^{-1}	assumed
k_4	0.4	day^{-1}	[47]
k_{12}	0.0008	$(\mathsf{pg}/M_I)/\mathsf{day}$	[47]
$k_{\alpha\beta}$	0.0029	$(\mathsf{pg}/A_{I,P})/\mathsf{day}$	[47]
k_γ	0.02	$(\mathsf{pg}/N_{\mathsf{at}})/\mathsf{day}$	[47]
$K_{\alpha\beta}$	75	$\mathsf{pg/mL}$	[34]
K_{12}	75	$\mathsf{pg/mL}$	[34]
K_γ	75	$\mathsf{pg/mL}$	[34]
μ_{12}	1.188	day^{-1}	[47]
$\mu_{\alpha\beta}$	2.77	day^{-1}	[47]
μ_γ	3	day^{-1}	[47]
k_Q	0.77	$(\mathsf{pg/mL})^{-1}/\mathsf{day}$	calculated
K_Q	3.63838	$\mathsf{pg/mL}$	calculated
μ_H	1.28	day^{-1}	[8]
k_B	0.6	$(\mathsf{pg/mL})^{-1}/\mathsf{day}$	calculated
K_B	4	$\mathsf{pg/mL}$	assumed
ρ_H	8.415×10^{-5}	$(\mathsf{pg/virion})/\mathsf{day}$	calculated
ρ_N	1.5×10^{-7}	$\mathsf{pg}/N_{\mathsf{at}}$	calculated
δ_M	0.0346	day^{-1}	calculated
θ	400	$\mathsf{pg/mL}$	assumed
m, n	2		

Table 2: Table with the description of the parameters used in the numerical simulation of differential equations. We added the references for the parameters used in the numerical simulation of differential equations.

IC's	Value	Range	Units	References
$A_0(0)$	4×10^5		A_0/mL	[50]
$A_I(0)$	1		A_I/mL	
$A_P(0)$	1		A_P/mL	
$V_{\mathsf{free}}(0)$	10^6	$[600, 10^6]$	$V_{\mathsf{free}}/\mathsf{mL}$	[50]
$V_{\mathsf{int}}(0)$	10		$V_{\mathsf{free}}/\mathsf{mL}$	[50]
$N_{\mathsf{in}}(0)$	3×10^5		$N_{\mathsf{in}}/\mathsf{mL}$	[38]
$N_{\mathsf{at}}(0)$	0		$N_{\mathsf{at}}/\mathsf{mL}$	–
$M_0(0)$	10^6		M_0/mL	[34]
$M_I(0)$	1		M_I/mL	[34]
$I_{12}(0)$	6	$[0 - 9.5]$	pg/mL	[43]
$I_{\alpha\beta}(0)$	20	$[0 - 20]$	pg/mL	[41]
$I_{\gamma}(0)$	30	$[0 - 60]$	pg/mL	[41]

Table 3: Initial conditions used in the simulations.

References

[1] Meijuan Zheng et al. *Functional exhaustion of antiviral lymphocytes in COVID-19 patients*. Cellular & Molecular Immunology https://doi.org/10.1038/s41423-020-0402-2

[2] Pascale André et al. *Anti-NKG2A mAb Is a Checkpoint Inhibitor that Promotes Anti-tumor Immunity by Unleashing Both T and NK Cells*. 2018, Cell 175, 1731-1743 December 13, 2018. Published by Elsevier Inc. https://doi.org/10.1016/j.cell.2018.10.014

[3] John B. Haanen and Vincenzo Cerundolo, *NKG2A, a New Kid on the Immune Checkpoint Block*. Cell 175, December 13, 2018, Elsevier Inc.

[4] Fadai NT, Sachak-Patwa R, Byrne HM, Maini PK, Bafadhel M, Nicolau Jr DV. *Infection, inflammation and intervention: mechanistic modelling of epithelial cells in COVID-19*. Journal of the Royal Society Interface. 2021;18(175):20200950.

[5] Ramakrishnan S, Nicolau Jr DV, Langford B, Mahdi M, Jeffers H, Mwasuku C, Krassowska K, Fox R, Binnian I, Glover V, Bright S. *Inhaled budesonide in the treatment of early COVID-19 (STOIC): a phase 2, open-label, randomised controlled trial*. The Lancet Respiratory Medicine. 2021.

[6] Yu LM, Bafadhel M, Dorward J, Hayward G, Saville BR, Gbinigie O, Van Hecke O, Ogburn E, Evans PH, Thomas NP, Patel MG. I*nhaled budesonide for COVID-19 in people at higher risk of adverse outcomes in the community: interim analyses from the PRINCIPLE trial.* medRxiv. 2021.

[7] Hagit Achdout, Irit Manaster, and Ofer Mandelboim, *Influenza Virus Infection Augments NK Cell Inhibition through Reorganization of Major Histocompatibility Complex Class I Proteins*. Journal of Virology, Aug. 2008, p. 8030-8037.

[8] Indrajit Ghosh, *Within host dynamics of SARS-CoV-2 in humans: Modeling immune responses and antiviral treatments* https://arxiv.org/abs/2006.02936v2

[9] Stephen N. Waggoner et al. *Roles of natural killer cells in antiviral immunity*. Curr Opin Virol. 2016 February ; 16: 15-23. https://doi:10.1016/j.coviro.2015.10.008.

[10] Elisabeth A. van Erp et al. *Viral Infection of Human Natural Killer Cells*. Viruses 2019, 11, 243; https://doi:10.3390/v11030243.

[11] Santosh Kumar, *Natural killer cell cytotoxicity and its regulation by inhibitory receptors*. 2018 John Wiley & Sons Ltd, Immunology, 154, 383-393.

[12] Abul K. Abbas, Andrew H. Lichtman, Shiv Pillai, *Cellular and Molecular Immunology*, 8th edition, Elsevier 2018.

[13] Judith A. Owen, Jenni Punt, Sharon A. Stranford, *KUBY Immunology*, 7nd edition, W. H. Freeman and Company, New York.

[14] Drew M. Pardoll, *The blockade of immune checkpoints in cancer immunotherapy*, Nature Reviews, Cancer, Vol. 12, 2012.

[15] Kenneth Murphy, Casey Weaver, *Janeway's immunobiology.* 9th edition. New York, NY: Garland Science/Taylor & Francis.

[16] Hagit Achdout, Irit Manaster, and Ofer Mandelboim, I *Influenza Virus Infection Augments NK Cell Inhibition through Reorganization of Major Histocompatibility Complex Class I Proteins.* JOURNAL OF VIROLOGY, Aug. 2008, p. 8030-8037.

[17] Thorbald van Hall et al. *Monalizumab: inhibiting the novel immune checkpoint NKG2A.* Journal for ImmunoTherapy of Cancer (2019) 7:263 https://doi.org/10.1186/s40425-019-0761-3

[18] Cristina Cerboni et al. *Antigen-activated human T lymphocytes express cell-surface NKG2D ligands via an ATM/ATR-dependent mechanism and become susceptible to autologous NK-cell lysis.* Prepublished online as Blood First Edition paper, April 3, 2007; https://doi:10.1182/blood-2006-10-052720.

[19] Amber M. Smith and Alan S. Perelson, *Influenza A virus infection kinetics: quantitative data and models.* Syst Biol Med 2011 3 429-445 https://doi:10.1002/wsbm.129.

[20] Eakachai Prompetchara, Chutitorn Ketloy, Tanapat Palaga, *Immune responses in COVID-19 and potential vaccines: Lessons learned from SARS and MERS epidemic.* Asian Pac J Allergy Immunol https://doi:10.12932/AP-200220-0772

[21] C. Zhang, Z. Wu and J.-W. Li et al., *The cytokine release syndrome (CRS) of severe COVID-19 and Interleukin-6 receptor (IL-6R) antagonist Tocilizumab may be the key to reduce the mortality*, International Journal of Antimicrobial Agents, https://doi:10.1016/j.ijantimicag.2020.105954

[22] *Instruction of Tocilizumab* https://www.gene.com/download/pdf/actemra_prescribing.pdf.

[23] Xiaoling Xu, Mingfeng Han, Tiantian Li, et al., *Effective Treatment of Severe COVID-19 Patients with Tocilizumab.* http://chinaxiv.org/abs/202003.00026.

[24] Ahmed Yaqinuddina and Junaid Kashirab, *Innate immunity in COVID-19 patients mediated by NKG2A receptors, and potential treatment using Monalizumab, Cholroquine, and antiviral agents*, Medical Hypotheses Volume 140, July 2020, https://doi.org/10.1016/j.mehy.2020.109777.

[25] Giuseppe Magro, *COVID-19: Review on latest available drugs and therapies against SARS-CoV-2. Coagulation and inflammation cross-talking.* Virus Research 286 (2020) https://doi.org/10.1016/j.virusres.2020.198070.

[26] Fabrizio De Benedetti, *Anti-IFN-γ Therapy for Cytokine Storm Syndromes* September 2019 DOI: 10.1007/978-3-030-22094-5/33. In book: Cytokine Storm Syndrome (pp.569-580), Randy Q. Cron and Edward M. Behrens Editors. Springer 2019.

[27] Chen LYC, Hoiland RL, Stukas S, et al. *Confronting the controversy: Interleukin-6 and the COVID-19 cytokine storm syndrome*. Eur Respir J 2020; in press https://doi.org/10.1183/13993003.03006-2020.

[28] Tang Y, Liu J, Zhang D, Xu Z, Ji J and Wen C (2020), *Cytokine Storm in COVID-19: The Current Evidence and Treatment Strategies*. Front. Immunol. 11_1708. https://doi.org/10.3389/fimmu.2020.01708.

[29] E.O. Gubernatorova, E.A. Gorshkovaa, A.I. Polinovaa, M.S. Drutskaya, *IL-6: Relevance for immunopathology of SARS-CoV-2*. Cytokine and Growth Factor Reviews 53 (2020) 13-24. https://doi.org/10.1016/j.cytogfr.2020.05.009

[30] Eric A. Coomes and Hourmazd Haghbayan, *Interleukin-6 in Covid-19: A systematic review and metaanalysis*. Rev Med Virol. 2020; e2141. wileyonlinelibrary.com/journal/rmv, 2020 John Wiley & Sons, https://doi.org/10.1002/rmv.2141.

[31] Hunter, C., Jones, S. *IL-6 as a keystone cytokine in health and disease*. Nat Immunol 16, 448-457 (2015),https://doi.org/10.1038/ni.3153.

[32] DeFranco, Locksley & Robertson: *Immunity. The Immnune Response in Infections and Inflammatory Disease*. Oxford U Press, Primers in Biology, 2007

[33] Ryo Otsuka and Ken-ichiro Seino. *Macrophage activation syndrome and* COVID-19. Inflammation and Regeneration (2020) 40:19. https://doi.org/10.1186/s41232-020-00131-w

[34] Judy Daya, Avner Friedman, and Larry S. Schlesinger. *Modeling the immune rheostat of macrophages in the lung in response to infection*. PNAS, July 7, 2009, vol. 106, no. 27, pag 11246-11251. www.pnas.org/cgi/doi/10.1073/pnas.0904846106

[35] Lee A. Segel and Leah Edelstein-Keshet. *A Primer on Mathematical Models in Biology* Society for Industrial and Applied Mathematics, 2013. ISBN: 1611972493.

[36] Amber M. Smith and Alan S. Perelson. *Influenza A virus infection kinetics: quantitative data and models*. 2010 John Wiley & Sons, Inc. WIREs Syst Biol Med 2011 3 429-445. DOI: 10.1002/wsbm.129

[37] Andreas Handel, Ira M. Longini Jr and Rustom Antia. *Towards a quantitative understanding of the within-host dynamics of influenza A infections*. J. R. Soc. Interface (2010) 7, 35-47. Published online 27 May 2009. doi:10.1098/rsif.2009.0067

[38] Xuefang Li and Jian-Xin Xu. *A mathematical model of immune response to tumor invasion incorporated with danger model*. Journal of Biological Systems, August 11, 2015, vol. 23, no.3, pag 505-526

[39] Frederik Graw and Alan S. Perelson. *Modeling Viral Spread*. Annual Reviews, August 31, 2016

[40] Pengxing Cao and James M. McCaw. *The mechanisms for within-host influenza virus control affect model-based assessment and prediction of antiviral treatment*. MDPI, July 26, 2017

[41] *CYPAN: Cytokien Panel, Plasma* `https://www.mayocliniclabs.com/test-catalog/Clinical+and+Interpretive/610259`..

[42] X.Xu, M. Han, T. Li, W. Sun, D. Wang, B. Fu, Y. Zhou, X. Zheng, Y. Yang, X. Li, X. Zhang, A. Pan and H. Wei *Effective treatment of severe COVID-19 patients with tocilizumba*. PNAs, May 19, 2020, vol. 11, no. 20, pag. 10970-10975

[43] G. Marzulli, G. Martemucci, A. Tafaro, A. G. D'Alessandro *Donkey and goat milk intake and modulation of the human aged response*. Current Pharmaceutical Design, March, 2010

[44] S. Baral, R. Antia and N. M. Dixit *A dynamical motif comprising the interactions between antigens and CD8 T cells may underlie the outcomes of viral infections*. PNAS, August 27, 2019, vol. 116, no. 35, pag. 17393-17398

[45] A. Radunskaya, R. Kim, T. Woods II. *Mathematical modeling of tumor immune interactions: A closer look at the role of a PD-L1 inhbitor in cancer immunotherapy*. Spora: A Journal of Biomathematics, 2018, vol. 4, issue 1, article 3

[46] Laetitia Canini and Fabrice Carrat *Population modeling of influenza A/H1N1 virus kinetics and symptom Dynamics*. Journal of Virology, March, 2011

[47] Simeone Marino and Denise E. Kirschner *The human immune respons to Mycobacterium tuberculosis lung and lymph node*. Journal of Theoretical Biology, November 17, 2003

[48] A. Friedman, J. Turner and B. Szomolay *A model on the influence of age on immunity to infection with Mycobacterium tuberculosis*. Exp Gerontol, April, 2008, vol. 43, no. 4, pag. 275-285

[49] M. A. Benchaid, A. Boucnhita, V. Volpert and A. Makhoute *Mathematical modeling reveals that the administration of EGF can promote the elimination of lymph node metastases by PD-1/PD-L1 blockade*. Front. Bioeng.Biotecnhol., May 14, 2019

[50] P. Baccam, C. Beauchemin, C. A. Macken, F. G. Hayden and A. S. Perelson *Kinetics of influenza A virus infection in humans*. Journal of Virology, August, 2016, pag. 7590-7599

[51] B. Hancioglu, D. Swigon and G. Clermont *A dynamical model of human immune response to infleunza A virus infection*. Journal of Theoretical Biology, December 11, 2006

[52] R. Brady, et al. *Personalized Mathematical Model Predicting Endotoxin-Induced Inflammatory Responses in Young Men.* https://arxiv.org/ftp/arxiv/papers/1609/1609.01570.pdf

[53] N. A. Awang and N. Maan *Analysis of tumor populations and immune system interaction model* Advances in Industrial and Applied Mathematics, AIP Publishing, 2016

[54] E. Mochan, E. Ackerman and J. E. Shoemaker *A systems and treatment perspective of models of influenza virus-induced host responses* Processes, 2018

[55] Daria Bortolotti, Valentina Gentili, ,Sabrina Rizzo, Antonella Rotola and Roberta Rizzo: *SARS-CoV-2 Spike 1 Protein Controls Natural Killer Cell Activation via the HLA-E/NKG2A Pathway.* Cells 2020, 9, 1975; doi:10.3390/cells9091975.

[56] Lai X, Friedman A (2017). *Combination therapy of cancer with cancer vaccine and immune checkpoint inhibitors: A mathematical model.* PLoS ONE 12(5): e0178479. https://doi.org/10.1371/journal.pone.0178479

[57] M. V. Gomez et al. *Kinetics and peptide dependency of the binding of the inhibitory NK receptor CD94/NKG2-A and the activating receptor CD94/NKG2-C to HLA-E.* The EMBO Journal, 1999, Vol.18, No.15, pp. 4250-4260

[58] Lucy C. Sullivan et. al *The heterodimeric assembly of the CD94-NKG2 receptor family and implications for human leukocyte antigen-E recognition* Elsevier, December, 2007

[59] Veronique M. Braud et. al *HLA-E binds to natural killer cell receptors CD94/NKG2A, B and C* Nature, 1998

[60] S. Sasmal, Y. Dong and Y. Takeuchi. *Mathematical modeling on t-cell mediated adaptive immunity in primary dengue infections.* Journal of theoretical biology, 2017

[61] A. Handel, I. M. Longini Jr and R. Antia *Towards a quantitative understanding of the within-host dynamics of influenza A infections.* Interface, May 27, 2009

[62] R. Keizer, A. Huitema, J. Schellens and J. Beijnen *Clinical Pharmacokinetics of Therapeutic Monoclonal Antibodies* Clin Pharmacokinet, 2010

[63] Y. M. Bar-On, A. Flamholz, S. Gleizer, B. Bernsthein, R. Phillips and R. Milo *SARS-CoV-2 (COVID-19) by the numbers.* eLife, 2020

[64] R. Sender, Y. M. Bar-On, A. Flamholz, S. Gleizer, B. Bernsthein, R. Phillips and R. Milo *The total number and mass of SARS-CoV-2 virions in an infected person*, medRxiv, 17 November, 2020

[65] E. A. H. Vargas and Jorge X Velasco-Hernandez *In-host modelling of covid-19 kinetics in humans.* medRxiv, 2020

[66] R. Ben-Shachar and Katia Koelle *Minimal within-host dengue models highlight the specific roles of the immune response in primary and secondary dengue infections*. Journal of the Royal Society Interface, 2015

[67] L. G. de Pillis, W. Gu and A. E. Radunskaya *Mixed immunotherapy and chemotherapy of tumors: modeling, applications and biological interpretations*. Elsevier, 2005

[68] Kimon V. Argyropoulos et. al *Association of Initial Viral Load in Severe Acute Respiratory Syndrome Coronavirus 2 (SARS-CoV-2) Patients with Outcome and Symptoms*. The American Journal Pathology, September 2020, Vol. 190, No. 9

[69] Fadai NT, Sachak-Patwa R, Byrne HM, Maini PK, Bafadhel M, Nicolau Jr DV. *Infection, inflammation and intervention: mechanistic modelling of epithelial cells in COVID-19*. Journal of the Royal Society Interface. 2021;18(175):20200950.

[70] Malik-Sheriff et al. *BioModels – 15 years of sharing computational models in life science*. Nucleic Acids Research. 2020 Jan, 48(D1):D407-415.